

Basic interaction operations for an underwater vehicle-manipulator system

Elisabetta Cataldi and Gianluca Antonelli

University of Cassino and Southern Lazio,

Via Di Biasio 43, 03043, Cassino, Italy,

E-mail: antonelli@unicas.it, e.cataldi@unicas.it

Abstract—In this paper an underwater vehicle-manipulator system is considered in order to accomplish two operations, namely to turn a valve and to push a button. Realistic assumptions, such as imperfect knowledge of the environment, have been considered with the purpose to design the proper interaction control scheme. In addition, due to the poor knowledge of the underwater dynamics, model-based approaches have been avoided. The UVMS is characterized by 13 Degrees-Of-Freedoms (DOFs) and a proper task-priority, inverse kinematics controller has been designed to take into account all the DOFs, however, this paper focuses on the interaction part. The redundancy exploitation is an ongoing activity being the interaction approach fully decoupled, and thus compatible, with the redundancy resolution scheme. The validation has been achieved resorting to a realistic mathematical model, including the main dynamic effects.

I. INTRODUCTION

Underwater operations by means of remotely or autonomous vehicle manipulator systems is an area of increasing research interest due to the great economical and social impact that it can affect. Among the various, operations interaction with the environment is critical to basic activities such as, for example, turning a valve of an deep oil& gas structure. Figure 1 shows a diver involved in an interaction operation.

From the control aspect, those operations require specific approaches. Several control schemes have been proposed in the literature, an overview of interaction control schemes can be found, e.g., in [1], [2].

One of the first underwater set-up aimed at interaction with the environment is a set-up composed by two 7-DOF Ansaldo manipulators to be used in cooperative mode [3]. The work [4] addresses control issue for an underwater vehicle carrying a manipulator in view of intervention missions. Recently, in [5] the Authors proposed an autonomous intervention robotic system



Fig. 1. Diver involved in an interaction operation.

aimed at learning the skills necessary to grasp and turn a valve. Underwater intervention received a boost with interesting results in the European project TRIDENT, see, e.g., [6], [7], and [8].

The Authors in [9] shown an autonomous intervention on an underwater environment, in the article some preliminary results in water tank conditions are presented by using the real mechatronics and the panel mockup, while in [10] the Authors have been shown their experiments architecture of the hardware in the loop.

This paper focuses in the implementation of two specific operations, namely to turn a valve and to push a button (see Figure 2). In the first operation, the system is required to rotate the valve around one axis, whilst in the second operation, it is required to impress a certain force on certain direction.

Interaction with a mobile base is a challenging problem also for aerial and ground robots. The Authors in [11] have presented some experiments with the purpose to turn a valve by resorting to a quadrotor equipped with two 2-DOFs arms. In [12] a wheeled-based mobile

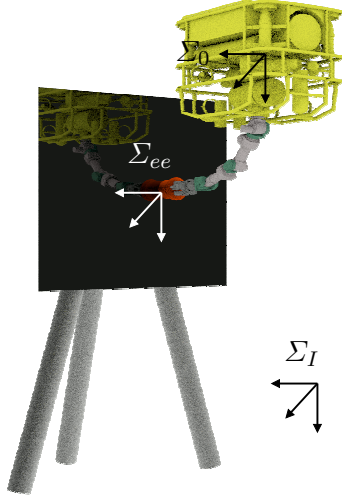


Fig. 2. Underwater vehicle-manipulator system pushing a button.

vehicle equipped with a manipulator is in charge of recognizing and pushing the buttons of an elevator.

The specific UVMS (Underwater Vehicle-Manipulator System) under investigation in this paper is a 13-DOF developed for the Italian National Project MARIS [13]. The interaction schemes is based on previous works [14], [15] and the validation has been achieved resorting to a realistic mathematical model, including the main dynamic effects.

II. MODELING

A. Kinematics

The vehicle is completely described by the position and orientation of a vehicle-fixed frame Σ_0 with respect to an earth-fixed inertial reference frame Σ_I as reported in Figure 2 together with the end-effector-fixed frame. Adapting the nomenclature in [16], the position of the vehicle-fixed frame is described by the vector $\eta_{p,0} = [x \ y \ z]^T \in \mathbb{R}^3$. The orientation of the vehicle-fixed frame is described by the (3×3) rotation matrix R_I^0 (rotation matrix expressing the transformation from the inertial frame to the vehicle-fixed frame). As customary in marine applications, the vehicle orientation is also represented in terms of the vector $\eta_{o,0} = [\phi \ \theta \ \psi]^T \in \mathbb{R}^3$ of Euler angles extracted from R_I^0 . The vehicle attitude in terms of quaternions will be denoted with $Q_0 = \{\eta_0, \varepsilon_0\}$.

Let us define $\eta_0 = [\eta_{p,0}^T \ \eta_{o,0}^T]^T$, and $\dot{\eta}_0 = [\dot{\eta}_{p,0}^T \ \dot{\eta}_{o,0}^T]^T$ the corresponding time derivatives. The vector $\nu_{p,0} \in \mathbb{R}^3$ is the linear velocity of the vehicle-fixed frame with respect to the inertial frame expressed in the vehicle-fixed frame and the vector $\nu_{o,0} \in \mathbb{R}^3$ is the

angular velocity of the vehicle-fixed frame with respect to the inertial frame expressed in the vehicle-fixed frame; $\nu_0 = [\nu_{p,0}^T \ \nu_{o,0}^T]^T$.

Let $q = [q_1 \ \dots \ q_n]^T \in \mathbb{R}^n$ be the vector of joint positions where n is the number of joints. The vector $\dot{q} \in \mathbb{R}^n$ is the corresponding time derivative. Let also define $\zeta = [\nu_{p,0}^T \ \nu_{o,0}^T \ \dot{q}^T]^T$.

The defined velocities are related via the following relation:

$$\zeta = \begin{bmatrix} R_I^0 & O_{3 \times 3} & O_{3 \times n} \\ O_{3 \times 3} & T(R_I^0) & O_{3 \times n} \\ O_{n \times 3} & O_{n \times 3} & I_{n \times n} \end{bmatrix} \begin{bmatrix} \dot{\eta}_{p,0} \\ \dot{\eta}_{o,0} \\ \dot{q} \end{bmatrix} = J_k(R_I^0) \begin{bmatrix} \dot{\eta}_{p,0} \\ \dot{\eta}_{o,0} \\ \dot{q} \end{bmatrix} \quad (1)$$

where $I_{n \times n}$ is the $(n \times n)$ identity matrix; $O_{n_1 \times n_2}$ is the $(n_1 \times n_2)$ null matrix; the matrix T can be found, e.g., in [1].

Position of the end effector is defined by the variable $\eta_{ee,p} \in \mathbb{R}^3$ while its orientation by $\eta_{ee,o} \in \mathbb{R}^3$ in terms of Euler angles and by $Q_{ee} = \{\eta_{ee}, \varepsilon_{ee}\} \in \mathbb{R}^4$ in terms of quaternions. The variable $\dot{\eta}_{ee}$ is the derivative of the end-effector position and ω_{ee} is the end-effector angular velocity.

The object fixed-frame is defined by $\Sigma_{obj} - x_{obj}y_{obj}z_{obj}$, for both the valve and button (see Figure 3). In particular, α_v is the angle around x_{obj} characterizing the valve position while the scalar x_b denotes the button position. The corresponding scalar velocities are ω_v and v_b .

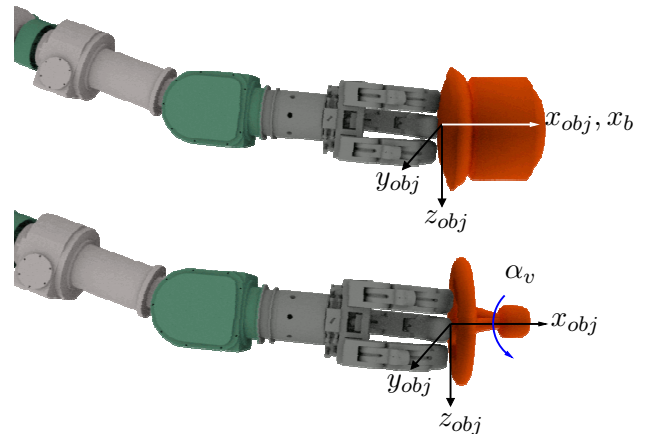


Fig. 3. Top: Button and End-effector positions, the white axis is the direction of desired the force. Bottom: Valve and End-effector positions, in this case the blue arc is the direction around which to rotate.

B. Dynamics

1) *Vehicle-Manipulator*: The dynamic model of an UVMS can be written in the following compact form [17], [18]:

$$\mathbf{M}(\mathbf{q})\dot{\boldsymbol{\zeta}} + \mathbf{C}(\mathbf{q}, \boldsymbol{\zeta})\boldsymbol{\zeta} + \mathbf{D}(\mathbf{q}, \boldsymbol{\zeta})\boldsymbol{\zeta} + \mathbf{g}(\mathbf{R}_I^0, \mathbf{q}) = \boldsymbol{\tau} \quad (2)$$

where $\mathbf{M}(\mathbf{q}) \in \mathbb{R}^{(6+n) \times (6+n)}$ is the inertia matrix including the added mass effects, $\mathbf{C}(\mathbf{q}, \boldsymbol{\zeta})\boldsymbol{\zeta} \in \mathbb{R}^{6+n}$ is the vector of Coriolis and centripetal terms including the added mass effects, $\mathbf{D}(\mathbf{q}, \boldsymbol{\zeta})\boldsymbol{\zeta} \in \mathbb{R}^{6+n}$ is the vector of friction and hydrodynamic damping terms (e.g., drag, lift, and vortex shedding generalized forces), $\mathbf{g}(\mathbf{R}_I^0, \mathbf{q}) \in \mathbb{R}^{6+n}$ is the vector of gravitational and buoyant generalized forces and $\boldsymbol{\tau} = [\boldsymbol{\tau}_v^T \ \boldsymbol{\tau}_q^T]^T \in \mathbb{R}^{6+n}$, is the vector composed by $\boldsymbol{\tau}_v \in \mathbb{R}^6$, (i.e., the forces and moments acting on the vehicle) and $\boldsymbol{\tau}_q \in \mathbb{R}^n$, (i.e., the manipulator's joint torques).

2) *Valve*: The valve is modelled by the equation:

$$J_v \dot{\omega}_v + \mu_v \omega_v = h_v \quad (3)$$

where J_v is the inertia around the rotation axis, i.e., x_{obj} , μ_v is the viscosity coefficient, ω_v is the angular velocity of the object-fixed frame around the rotation axis and h_v is the moment provided by the robotic system.

3) *Button*: The button is modelled as a spring-damper body, the equation is:

$$m_b \ddot{x}_b + \mu_b \dot{x}_b + k_b (x_b - x_0) = h_b \quad (4)$$

where m_b is the mass, μ_b is the viscosity coefficient, k_b is the compliance, x_b is the object-fixed position along x_{obj} , x_0 is the corresponding rest position and h_b is the force provided by the robotic system.

III. CONTROL PROBLEMS

Two case studies will be considered, labelled as *turn the valve* and *push the button* and briefly described here:

- **turn the valve**. The UVMS is assumed to already having grabbed the valve. The valve orientation is estimated with a maximum *polarized* error of 1.5 degrees. The mission is terminated when the valve has been rotated by 20.0 degrees.
- **push the button**. The UVMS is assumed to be in a configuration in which the end-effector exhibits its approaching direction perpendicular to a vertical plane (see figure 3). As said, the plane is compliant but its real orientation is assumed to be estimated with 15 degrees of error. Pushing

the button is achieved when a force of 200 N in the direction normal to the button is exerted for at least 10 seconds with an error bounded in $\pm 10\%$.

IV. INTERACTION CONTROLLERS

The interaction control architecture has been designed based on two levels, an external loop that controls the interaction force exchanged between the system and the environment, and an internal loop that manages both the inverse kinematics and direct dynamics. Intentionally, no model-based compensation is assumed.

The internal loop, common to both operations, is shown in Figure 4; it receives as input the desired end-effector position and orientation and the kinematic desired secondary tasks. The corresponding outputs are the desired vehicle and manipulator trajectories [18] sent to the dynamic controller. Remarkably, there are no constraints on the latter, one possibility is to control the vehicle by properly compensating the presence of the arm [19] and controlling the arm with a basic PID at joint approach.

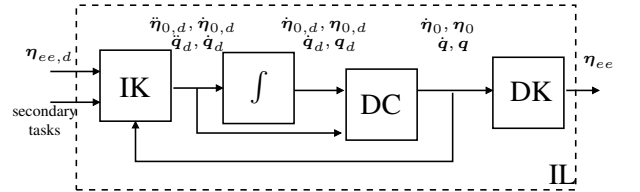


Fig. 4. *Internal Loop (IL)* : composed by the inverse kinematics (IK), the dynamic control (DC) and the direct kinematics (DK).

As said, the two operations are afforded by means of two different external loops, an impedance controller for the *turn a valve* operation and a force control for the *push a button*. It is known that interaction schemes may suffer from uncertainty in the estimation of the environmental geometry configuration, in such a case, in fact, the interaction arises in a direction where it was not planned for. While for the *turn a valve* operation this is not considered as a practical problem, it may be significant for explicit force control schemes. In the numerical simulations such uncertainty will be simulated. It is worth noticing that, in case needed, more sophisticated interaction control scheme may be easily adopted.

Figure 5 shows the impedance control for the *turn a valve* operation, based on a common architecture [1], [18]. This type of control is an indirect force control, because the interaction force is not directly regulated but the control objective is rather the desired end-effector impedance.

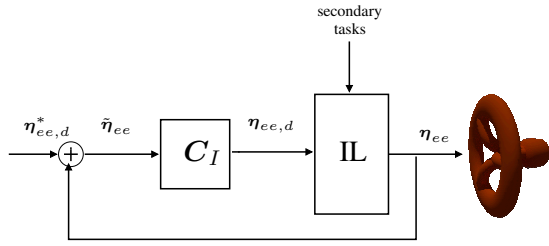


Fig. 5. *External Loop for turn a valve* : It is composed by the impedance control (C_I) and the internal loop (IL).

The impedance control inputs are the measured and the desired end-effector position and orientation. In this case our target is turn a valve, the end-effector is positioned perpendicular to the valve and our intention is to turn it around the x_{obj} -axis, as Figure 3 shows. The desired trajectories have been determined by the desired movement on the valve.

Its outputs are the desired values required from the internal loop. The control law used for the impedance control is:

$$\eta_{ee,d} = \mathbf{K}_S \tilde{\eta}_{ee} + \mathbf{K}_D \tilde{v}_{ee} + \mathbf{K}_I \int_{t_0}^t \tilde{\eta}_{ee}(\sigma) d\sigma,$$

where the matrices $\mathbf{K}_S, \mathbf{K}_D, \mathbf{K}_I \in \mathbb{R}^{6 \times 6}$ are respectively the stiffness, damping and integral gain matrix. We have added the integral term to ensure a null steady state error. Where the position error $\tilde{\eta}_{ee}$ is obtained from:

$$\tilde{\eta}_{ee} = \begin{bmatrix} \eta_{ee,p,d}^* - \eta_{ee,p} \\ \eta_{ee,\varepsilon^*,d} - \eta_{ee,\varepsilon} - \mathbf{S}(\varepsilon_{ee,d}^*) \varepsilon \end{bmatrix} \in \mathbb{R}^6,$$

where $\eta_{ee,p,d}^*$ and $Q_{ee,d}^* = \{\eta_{ee,\varepsilon,d}^*, \varepsilon_{ee,d}^*\}$ are the desired end-effector position and quaternion; and $\dot{\tilde{\eta}}_{ee}$ is given by:

$$\tilde{v}_{ee} = \begin{bmatrix} \dot{\eta}_{ee,p,d} - \dot{\eta}_{ee,p} \\ \omega_{ee,d} - \omega_{ee} \end{bmatrix}$$

in this case the variable $\dot{\eta}_{ee,p,d}$ is the time derivative of the desired end-effector position, while $\omega_{ee,d}$ is the desired end-effector velocity.

The external loop for the *push a button* operation is composed by the force control [1], [18]. A Proportional Integral action is used to stabilize the force error. In fact, being the force signal characterized by a strong noise, its time derivative is usually useless. The impedance loop thus provides a damping effect [1].

The force control law is:

$$\eta_{ee,d}^* = \mathbf{K}_P \tilde{h}_{ee} + \mathbf{K}_I \int_{t_0}^t \tilde{h}_{ee}(\sigma) d\sigma,$$

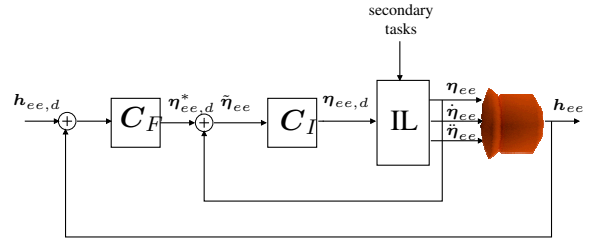


Fig. 6. *External Loop for push a button* : composed by the Force Control (C_F), the Impedance Control (C_I) and the Internal Loop (IL).

variables	T_s [Hz]
vehicle position	50
vehicle roll-pitch	50
vehicle yaw	50
joint position	50
e.e. force/moment	10^3
target configuration	10

TABLE I. SAMPLING TIMES OF THE MEASURED VARIABLES USED IN THE SIMULATION.

where the matrices \mathbf{K}_P and $\mathbf{K}_I \in \mathbb{R}^{6 \times 6}$ are respectively the proportional and integral gain matrix. Also here we have added the integral term to ensure a null steady state error. The force error \tilde{h}_{ee} is obtained from:

$$\tilde{h}_{ee} = h_{ee,d} - h_{ee} \in \mathbb{R}^6.$$

where h_{ee} are the forces and moments measured by the sensor put on the end-effector, whereas the desired forces and moments $h_{ee,d}$ are selected on the basis of the required forces and moments desired on the button.

V. NUMERICAL SIMULATION

Numerical simulations have been performed to validate the above approach. A realistic model, taking into account the most significant physical terms, has been derived. The underwater vehicle-manipulator system is composed by a full-DOF system, i.e., 6-DOF for the vehicle and 7-DOF for the arm. The dynamic parameters of the vehicle have been experimentally identified in [20] while the arm's parameters have been extrapolated by the CAD data and simple heuristic tests.

The numerical integration of the non linear differential equations of the closed loop systems have been achieved by resorting to Matlab and by properly adapting its tool SimMechanics. For each simulated sensor a different sampling time T_s has been used as shown in table I.

Axis	C_F		C_I		
	K_P	K_I	K_S	K_D	K_I
x	$4 \cdot 10^{-3}$	$7 \cdot 10^{-3}$	0.5	0.05	0.20
y	$4 \cdot 10^{-3}$	$7 \cdot 10^{-3}$	0.5	0.05	0.20
z	$4 \cdot 10^{-3}$	$7 \cdot 10^{-3}$	0.5	0.05	0.20
ϕ	$2 \cdot 10^{-3}$	$5 \cdot 10^{-3}$	0.2	0.1	0.15
θ	$2 \cdot 10^{-3}$	$5 \cdot 10^{-3}$	0.2	0.1	0.15
ψ	$2 \cdot 10^{-3}$	$5 \cdot 10^{-3}$	0.2	0.1	0.15

TABLE II. CONTROL GAINS, FOR THE FORCE CONTROL AND THE IMPEDANCE CONTROL.

Tuning of the parameters have been achieved with the following, pragmatic, procedure. By assuming that an existing industrial set-up is used, it is not possible and/or efficient to modify the dynamic controller of both the vehicle and the arm, this means that the inner control loop is given. Its outer control loop, the task-priority inverse-kinematics controller, is thus tuned with a bandwidth *slower* with respect to the dynamic loop, ideally, the kinematic loop should *see* as instantaneous the dynamic loop. A similar reasoning allowed to tune the outer control loop, i.e., the interaction one.

The chosen gains are reported in Table II, they are both the impedance and force control gains used during the simulations.

Figure 7 shows the valve orientation, a valve movement of 20 degrees in 10 seconds has been imposed to the system, we can appreciate that the valve follows the trajectory with a reasonable error.

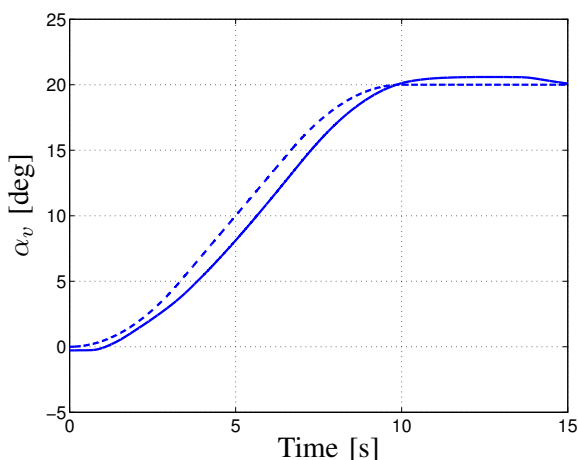


Fig. 7. Turn a valve: The desired (dashed-line) and simulated (solid-line) valve orientation along the x -axis.

The end-effector orientation (solid-line) and its de-

sired values (dashed-line) are shown in figure 8, in this figure we can appreciate that the end-effector moves only around the x -axis even if an error of the perception system has been simulated. In the other directions, the movements are smaller than the x -axis, it enforces that the valve has been modelled rigid in the y, z -axes.

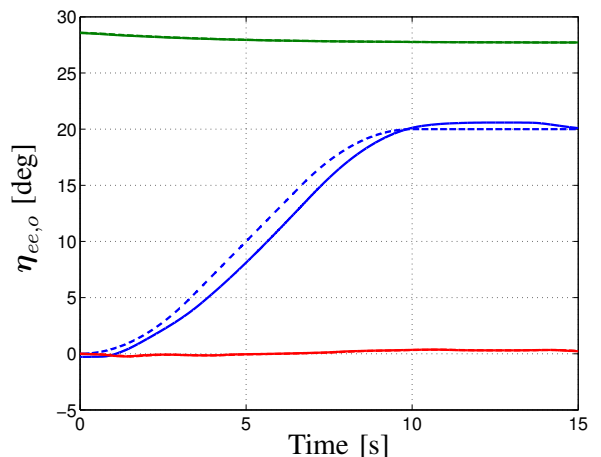


Fig. 8. Turn a valve: The simulated end-effector orientation (solid-line) of the x -axis (blue), y -axis (green) and z -axis (red) are reported, and their respectively desired orientation (dashed-line).

Figure 9 shows the desired (dashed-line) and simulated forces (solid-line) on the end-effector, we can view that the system completes the operation, and as we expected at the steady-state it has a null-error.

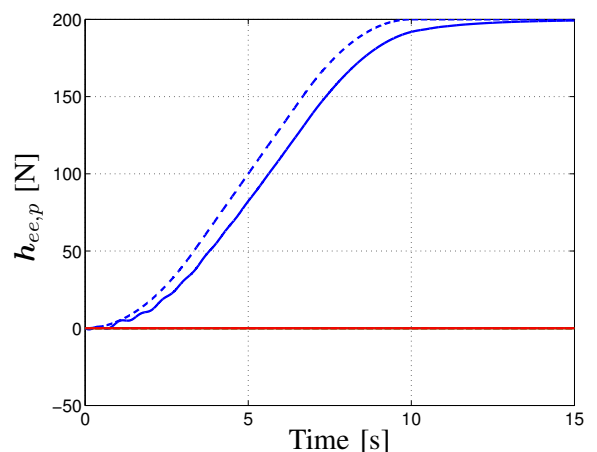


Fig. 9. Push a button: The simulated forces (solid-line) of the x -axis (blue), y -axis (green) and z -axis (red) are reported, and their respectively desired forces (dashed-line).

Figure 10 shows the desired (dashed-line) and the simulated (solid-line) end-effector position. It can be appreciated that the main movement of the end-effector is along the interaction direction. Along the plane parallel to the interaction plane, due to the intentional perception

error considered, we experience a small drift that can be ignored if it is compatible with the push-button operation or handle with more sophisticated force control strategies if needed.

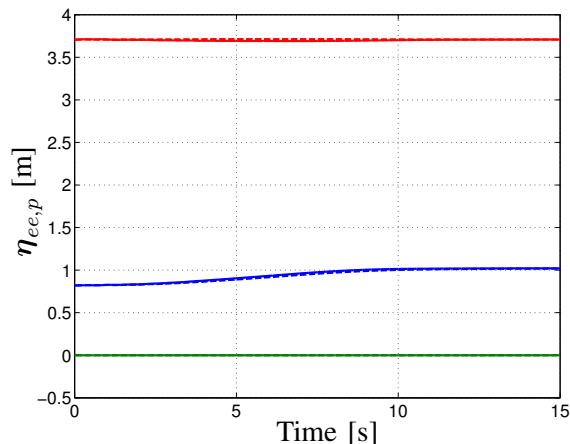


Fig. 10. *Push a button*: The simulated end-effector position (solid-line) of the x -axis (blue), y -axis (green) and z -axis (red) are reported, and their respectively desired position (dashed-line).

VI. CONCLUSIONS

In this paper we presented a control approach to accomplish two underwater operations, turn a valve and push a button, to be performed by an underwater vehicle-manipulator system. The presented control is composed by a two loop architecture, the inner loop presents the kinematics and dynamic control, whilst the external loop is the interaction control part. While the inner is the same for both operations, we implemented two different outer loop for the interaction. Numerical simulations on a realistic dynamic model prove the efficiency of the proposed strategy.

ACKNOWLEDGEMENTS

This research has received funding from the European Community's Seventh Framework Programme under grant agreement n. 287617 (IP project ARCAS - Aerial Robotics Co-operative Assembly system), n. 635491 (IP project DEXROV - Dexterous ROV Operations in Presence of Communications Latencies), n. 645141 (IP WiMUST - Widely Scalable Mobile Underwater Sonar Technology), and Italian *Ministero dell'Istruzione, dell'Università e della Ricerca, PRIN 2010-2011* with protocol 2010FBLHRJ (project MARIS - Marine Autonomous Robotics for InterventionS).

REFERENCES

- [1] B. Siciliano, L. Sciacivco, L. Villani, and G. Oriolo, *Robotics: modelling, planning and control*. Springer Verlag, 2009.
- [2] L. Villani and J. De Schutter, *Springer Handbook of Robotics*. Heidelberg, D: B. Siciliano, O. Khatib, (Eds.), Springer-Verlag, 2008, ch. Force Control.
- [3] G. Casalino, D. Angeletti, T. Bozzo, and G. Marani, "Dexterous underwater object manipulation via multi-robot cooperating systems," in *Robotics and Automation, 2001. Proceedings 2001 ICRA. IEEE International Conference on*, vol. 4. Seoul, Korea: IEEE, 2001, pp. 3220–3225.

- [4] G. Marani, S. Choi, and J. Yuh, "Real-time center of buoyancy identification for optimal hovering in autonomous underwater intervention," *Intelligent Service Robotics*, vol. 3, no. 3, pp. 175–182, 2010.
- [5] A. Carrera, S. R. Ahmadzadeh, A. Ajoudani, P. Kormushev, M. Carreras, and D. G. Caldwell, "Towards autonomous robotic valve turning," *Cybernetics and Information Technologies*, 2012.
- [6] J. Fernández, M. Prats, P. Sanz, J. C. García Sánchez, R. Marin, M. Robinson, D. Ribas, and P. Ridao, "Manipulation in the seabed: A new underwater robot arm for shallow water intervention," *IEEE Robotics & Automation Magazine*, 2013.
- [7] M. Prats, D. Ribas, N. Palomeras, J. García, V. Nannen, S. Wirth, J. Fernández, J. Beltrán, R. Campos, P. Ridao *et al.*, "Reconfigurable AUV for intervention missions: a case study on underwater object recovery," *Intelligent Service Robotics*, vol. 5, no. 1, pp. 19–31, 2012.
- [8] E. Simetti, G. Casalino, S. Torelli, A. Sperindé, and A. Turetta, "Floating underwater manipulation: Developed control methodology and experimental validation within the TRIDENT project," *Journal of Field Robotics*, vol. 31(3), pp. 364–385, 2013.
- [9] A. Peñalver, J. Pérez, J. J. Fernández, J. Sales, P. Sanz, J. Garcia, D. Fornas, and R. Marin, "Autonomous intervention on an underwater panel mockup by using visually-guided manipulation techniques?" in *World Congress*, vol. 19, no. 1, 2014, pp. 5151–5156.
- [10] P. Sanz, J. Perez, A. Penalver, J. Fernandez, D. Fornas, J. Sales, and R. Marin, "Grasper hil simulation towards autonomous manipulation of an underwater panel in a permanent observatory," in *Oceans - San Diego, 2013*, Sept 2013, pp. 1–6.
- [11] M. Orsag, C. Korpela, S. Bogdan, and P. Oh, "Valve turning using a dual-arm aerial manipulator," in *Unmanned Aircraft Systems (ICUAS), 2014 International Conference on*, May 2014, pp. 836–841.
- [12] K. Inoue, Y. Takao, T. Arai, and Y. Mae, "Presentation of push button switches with manipulators for virtual operating environment," in *Intelligent Robots and Systems, 2000. (IROS 2000). Proceedings. 2000 IEEE/RSJ International Conference on*, vol. 2, 2000, pp. 1137–1142 vol.2.
- [13] G. Casalino, M. Caccia, A. Caiti, G. Antonelli, G. Indiveri, C. Melchiorri, and S. Caselli, "MARIS: a national project on marine robotics for interventions," in *22th Mediterranean Conference on Control and Automation*, Palermo, I, June 2014.
- [14] G. Antonelli, S. Chiaverini, and N. Sarkar, "External force control for underwater vehicle-manipulator systems," *IEEE Transactions on Robotics and Automation*, vol. 17, no. 6, pp. 931–938, December 2001.
- [15] G. Antonelli, N. Sarkar, and S. Chiaverini, "Explicit force control for underwater vehicle-manipulator systems," *Robotica*, vol. 20, no. 3, pp. 251–260, 2002.
- [16] SNAME, "Nomenclature for treating the motion of a submerged body through a fluid," *Technical and Research Bulletin*, pp. 1–5, 1950.
- [17] I. Schjøllberg and T. Fossen, "Modelling and control of underwater vehicle-manipulator systems," in *in Proc. 3rd Conf. on Marine Craft maneuvering and control*, Southampton, UK, 1994, pp. 45–57.
- [18] G. Antonelli, *Underwater robots*, 3rd ed. Heidelberg, D: Springer Tracts in Advanced Robotics, Springer-Verlag, January 2014.
- [19] G. Antonelli and E. Cataldi, "Recursive adaptive control for an underwater vehicle carrying a manipulator," in *Control and Automation (MED), 2014 22nd Mediterranean Conference of*, June 2014, pp. 847–852.
- [20] M. Caccia, G. Indiveri, and G. Veruggio, "Modeling and identification of open-frame variable configuration unmanned underwater vehicles," *Oceanic Engineering, IEEE Journal of*, vol. 25, no. 2, pp. 227–240, 2000.